J Mater Sci: Mater Electron (2013) 24:2135–2140
DOI 10.1007/s10854-013-1071-z

Effect of crystallizable glass addition on sintering and dielectric behaviors of barium titanate ceramics

Xiaofeng Su · Minoru Tomozawa · J. Keith Nelson · Douglas B. Chrisey

Received: 23 November 2012 / Accepted: 11 January 2013 / Published online: 25 January 2013

Abstract A crystallizable glass which can precipitate barium titanate was added to $BaTiO_3$ ceramics to study its effect on sintering behavior and dielectric properties of the composites. High densification (>95 % theoretical density) was achieved by addition of glass phase and the dielectric constant of composites was enhanced through the crystallization of glass phase. A composite with 90 wt% $BaTiO_3$ and 10 wt% glass showed a dielectric constant of ~2,300 at room temperature at 1 kHz and a dielectric breakdown strength about 140 kV/cm.

1 Introduction

Barium titanate ($BaTiO_3$) has been widely studied as a dielectric for commercial energy storage capacitors due to its high dielectric constant [1–3]. However, the dielectric breakdown strength of polycrystalline bulk $BaTiO_3$ ceramic is relatively low (~100 kV/cm) [4]. In order to achieve a high energy storage value by a capacitive approach, both high dielectric constant (ε_r) and high dielectric breakdown strength (E_b) are necessary. Recently, numerous studies have been conducted to investigate the effects of glass addition on $BaTiO_3$, especially on sintering and electrical properties of composites [5, 6]. Many benefits can be expected by adding glass to ceramics, including reduction of the porosity and the sintering temperature, refinement of microstructures and improvement of some electrical properties. Hsiang et al. [7] reduced the sintering temperature of $BaTiO_3$ from 1,300 to 900 °C by using a $ZnO–B_2O_3–SiO_2$ (ZBS) glass as the sintering agent. Lower sintering temperature is not only beneficial to decrease processing cost but also allows for the usage of base metal electrodes such as copper and nickel [8]. Due mainly to the reduction of the sintering temperature, abnormal grain growth of $BaTiO_3$ was prevented by the addition of $Mn_2O_3–SiO_2$ glass [9]. Moreover, the added glass can improve dielectric breakdown strength of composites significantly. Young [10] used $BaO–SrO–SiO_2–Al_2O_3–B_2O_3–ZrO_2$ glass to sinter $BaTiO_3$ and investigated the influence of glass addition on the dielectric breakdown strength of $BaTiO_3$. The dielectric breakdown strength of samples with 20 vol% glass was found to become higher by a factor of 2.8 compared to that of the pure $BaTiO_3$. In addition, it was demonstrated that capacitance temperature stability can be also enhanced by adding calcium borosilicate glass to $BaTiO_3$ based ceramics [11]. However, the addition of glass phase often deteriorates the dielectric constant of composite drastically, especially when the loading of glass phase is over 10 wt% [5, 12]. An addition of 13 wt% lead borate glass was found to decrease the dielectric constant from above 2,000 to around 1,000 [5]. Previous work [13] demonstrated that this low dielectric permittivity is undesirable for high energy density application.

Herein, we consider another approach to maintain the high dielectric constant of $BaTiO_3$/glass composite. A crystallizable glass is used as a sintering agent for $BaTiO_3$ ceramics. Some glasses can precipitate $BaTiO_3$ phase upon a subsequent crystallization heat-treatment [14] after

X. Su · M. Tomozawa (✉) · D. B. Chrisey
Department of Materials Science and Engineering, Rensselaer Polytechnic Institute, Troy, NY 12180, USA
e-mail: tomozm@rpi.edu

J. K. Nelson
Department of Electrical, Computer and Systems Engineering, Rensselaer Polytechnic Institute, Troy, NY 12180, USA

D. B. Chrisey
Department of Physics and Physical Engineering, Tulane University, New Orleans, LA 70118, USA

sintering process. This paper provides a new approach to keep the benefits of glass sintering aid without sacrificing high dielectric constant of $BaTiO_3$. The effect of crystallizable glass addition on sintering behavior and dielectric properties was studied.

2 Experimental procedure

2.1 Glass fabrication and characterization

Glass with the composition (34.2 mol% BaO–35.8 mol% TiO_2–20 mol% SiO_2–10 mol% Al_2O_3) was prepared by a conventional glass melting technique. First, reagent grade $BaCO_3$, TiO_2, SiO_2 and Al_2O_3 powders were mixed thoroughly and melted in a platinum crucible at 1,450 °C for 2 h. The melt was cast onto a preheated stainless steel plate and the resulting transparent glass was transferred to an annealing furnace. Glass powder was prepared by grinding the glass in an agate mortar with pestle. Differential thermal analysis (DTA) of BaO–TiO_2–SiO_2–Al_2O_3 glass powder was performed using a DTA analyzer (STA 409C/CD, NETZSCH, Selb, Germany) with a heating rate of 10 °C/min in helium atmosphere. Crystallization of glass powder upon heating was investigated by in situ X-ray diffraction (XRD) using a diffractometer (X'pert Pro., PANalytical, Almelo, Netherland) with Cu Kα radiation (λ = 1.5406 Å). The heating rate was 10 °C/min with a dwell time of 15 min at selected temperatures.

2.2 Pellet preparation

The glass powder was mixed with $BaTiO_3$ powder (<100 nm particle size, ≥99 % in purity, Sigma-Aldrich Co., USA) using agate mortar and pestle at glass weight percents of 10, 15 and 20. The mixtures were designated as BG10, BG15 and BG20 (the corresponding glass volume percentages were 13.4, 19.8, and 25.9 vol% respectively). The mixture powder was added with 4 wt% polyvinyl alcohol (PVA) solution and pressed into pellets with 13 mm diameter and 0.4 mm thickness by applying 6,000 lbs load for 1 min. Pellets were sintered at 1,200 °C for 4 h in air and given crystallization heat-treatment at 1,000 °C for 2 h followed by furnace cooling.

2.3 Characterization of pellets

The density of pellets after heat-treatment was measured by the Archimedes method. Microstructure investigation of composites was performed using a high resolution field emission scanning electron microscope (SUPRA 55, Carl Zeiss Microscopy LLC, Thornwood, NY, USA). Crystal phases of samples were studied by using the X-ray diffractometer. Silver electrodes of 6 mm diameter were painted on both sides of pellets and dried at room temperature overnight. The dielectric properties (dielectric constant and loss tangent) were characterized by a RLC Digibridge (RLC 1689 Tester, IET Labs Inc., Westbury, NY, USA) with a frequency range from 100 Hz to 100 kHz at temperatures from room temperature to 150 °C. The DC dielectric breakdown voltage of pellets was measured at room temperature using the Hipotronics high voltage DC power supply (Hipotronics Inc., Brewster, NY, USA). Pellets were immersed in silicone oil to avoid surface flashover. Approximately 10 pellets for each composition were measured with the voltage ramp rate of approximately 10 kV/min. The accurate sample thickness was measured by an optical microscope observation of its cross-section after the breakdown voltage measurements to obtain the dielectric breakdown strength in kV/cm.

3 Results

3.1 Glass characterization

The DTA result of glass powder shown in Fig. 1 was analyzed to obtain the glass transition temperature of ~735 °C, crystallization initiation temperatures of T_{x1} = 835 °C and T_{x2} = 958 °C, and melting temperature of ~1,200 °C. Crystallization and phase evolution processes of glass powder were also observed by in situ X-ray diffraction pattern as shown in Fig. 2. At room temperature (25 °C), the broad peak demonstrated the amorphous nature of glass powder. When temperature reaches 850 °C, BaO and TiO_x phases precipitated first which contribute to the first exothermal peak of DTA curve at around 835 °C. With further increasing temperature, BaO and TiO_x peaks decreased while $BaTiO_3$ and $BaAl_2Si_2O_8$ phases precipitated, resulting in the second exothermal peak of DTA at 958 °C. At 1,000 °C, $BaTiO_3$ is the primary crystallized phase, accompanied by the secondary phase $BaAl_2Si_2O_8$. Therefore, in order to precipitate $BaTiO_3$ phase in this glass, heat-treatment around 1,000 °C is necessary.

3.2 Liquid phase sintering and crystallization

The theoretical density of $BaTiO_3$ was taken as 6.02 g/cm^3 [15], while that of glass component with precipitated $BaTiO_3$ was estimated, by measuring the density of pore-free pure glass plates after crystallization heat-treatment at 1,000 °C for 2 h, as 4.32 g/cm^3. The theoretical density of composites can be calculated using a linear mixing rule. Relative densities of three composites are shown in Fig. 3 (BG10 95.8 %, BG15 96.6 % and BG20 97.0 %). High densification of greater than 95 % theoretical density was

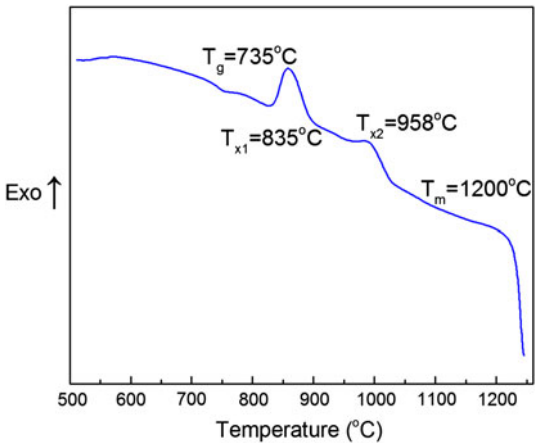

Fig. 1 Differential thermal analysis of the crystallizable glass, $34.2BaO–35.8TiO_2–20SiO_2–10Al_2O_3$ (mol%)

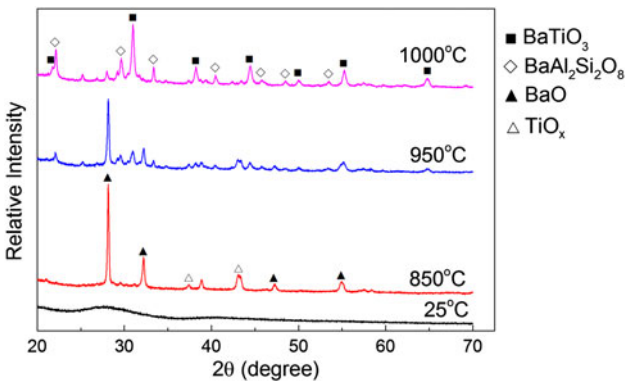

Fig. 2 In-situ X-ray diffraction pattern of the glass powder (intensities are displaced for clarity)

achieved for all composites, with the highest percent theoretical density being obtained for the composite with the largest volume fraction of glass component. It appears that densification is promoted with increasing glass additions since glass can fill the air-filled pores of ceramics while sintering. The scanning electron micrographs of heat-treated composites with different amount of glass component from 10 to 20 wt% are shown, together with that of as-received $BaTiO_3$, in Fig. 4. As-received $BaTiO_3$ nanopowder had nearly uniform grain size with the average value of 50 nm in diameter. $BaTiO_3$/glass composites with 10 wt% glass have fine microstructures as shown in Fig. 4b. Composite pellets containing 15 or 20 wt% glass showed larger grain size of approximately several hundred nanometers with highly densified microstructure.

XRD patterns of the three composites are shown in Fig. 5 in semi-log plot to accentuate the minor crystalline components. Since the composite samples contain 80 wt% or more $BaTiO_3$, their diffraction peaks in the XRD pattern are dominated by those of $BaTiO_3$. The primary precipitated phase of glass upon heat-treatment at 1,000 °C for 2 h

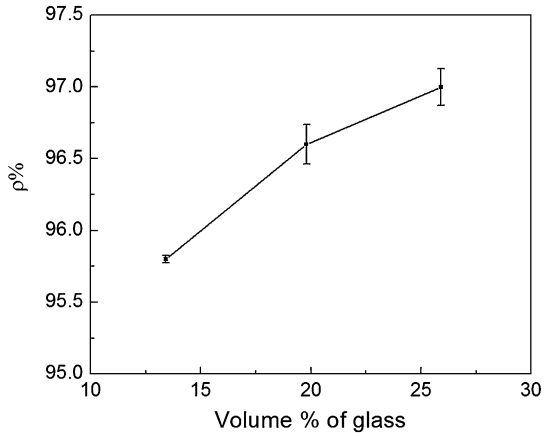

Fig. 3 Relative density (% theoretical density) of BG10 (90 wt% $BaTiO_3$–10 wt% Glass), BG15 (85 wt% $BaTiO_3$–15 wt% Glass) and BG20 (80 wt% $BaTiO_3$–20 wt% Glass)

was also $BaTiO_3$ as shown in Fig. 2. Thus, it is difficult to characterize crystallization process of glass phase in composites by the normal XRD plot. However, small peaks due to $BaAl_2Si_2O_8$ phase can be observed in the semi-log plot of Fig. 5. Figure 2 showed that secondary phase $BaAl_2Si_2O_8$ precipitated simultaneously with primary phase $BaTiO_3$. Thus, $BaAl_2Si_2O_8$ peaks in the XRD semi-log plot of Fig. 5 is an indication of crystallization of the glass component during heat-treatment of the composite samples.

3.3 Dielectric permittivity and dielectric breakdown strength

Figure 6 shows (a) relative permittivity (dielectric constant) and (b) loss tangent of three composites at 1 kHz as a function of temperature. The dielectric constant decreased with increasing fraction of added glass. The broad peaks around 130 °C of three composites resulted from the ferroelectric transition of $BaTiO_3$. The peak positions (Curie temperature T_C) of three composites remained unchanged within the experimental error in this work. The peak diffuseness changed with glass addition, with BG10 having the sharpest peak and BG20 the broadest one in terms of the full width at half maximum (FWHM) normalized by peak height. Bae et al. [16] showed that diffusive phase transition contributed to the nearly temperature-independent dielectric constant, which is desirable in applications of multilayer ceramic capacitors. The loss tangent of three composites decreased with increasing temperature and most values are below 0.01 in the temperature range of 40–150 °C. Figure 7 presents the temperature coefficient of capacitance (TCC) of three composites at 1 kHz over the temperature range of 22–150 °C. All TCCs are within ±15 % for BG15 and BG20, while the TCC value at T_C for BG10 is around 20.0 %.

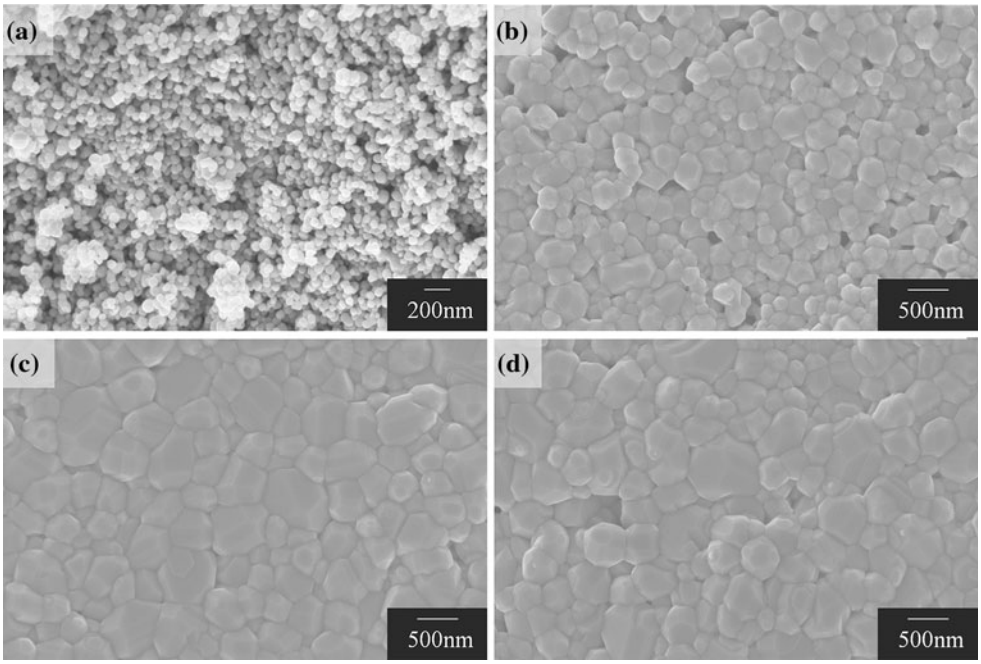

Fig. 4 Scanning electron micrographs of **a** as-received $BaTiO_3$ nanopowder, **b** BG10 (90 wt% $BaTiO_3$–10 wt% Glass), **c** BG15 (85 wt% $BaTiO_3$–15 wt% Glass), and **d** BG20 (80 wt% $BaTiO_3$–20 wt% Glass) after sintering and crystallization heat-treatment

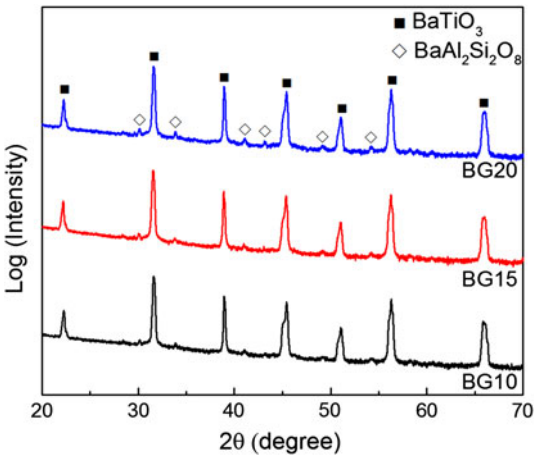

Fig. 5 Semi-log plot of XRD patterns for three composites (intensities are displaced for clarity)

Figure 8 is the Weibull plot of dielectric breakdown strength for three composites. Weibull distribution is generally applied for dielectric breakdown analysis, which can be described as,

$$F = 1 - \mathrm{Exp}\left[-\left(\frac{E_i}{\alpha}\right)m\right] \quad (1)$$

$$\ln[-\ln(1-F)] = m\ln E_i - m\ln\alpha \quad (2)$$

$$F = \frac{i}{n+1} \quad (3)$$

$$E_1 \le E_2 \le \cdots \le E_i \le \cdots \le E_n \quad (4)$$

where F is failure probability, E_i is the dielectric breakdown strength value of the ith sample when the strength is arranged in the ascending order, n is the total number of sample measured, m is the distribution parameter, with a larger m value indicating a narrower distribution and α is a constant which indicates the value of characteristic dielectric breakdown strength of the material.

There will be a linear relationship between $\ln E_i$ and $\ln(-\ln(1-F))$ as shown in Fig. 8. The value of m can be obtained by the slope and dielectric breakdown strength at 63.2 % failure probability is defined as the characteristic dielectric breakdown strength of each composite. Figure 8 shows that the distribution of breakdown strength for BG15 ($m = 12.4$) and BG20 ($m = 8.1$) are narrower than that of BG10 ($m = 3.8$). BG10 exhibited a characteristic dielectric breakdown strength of 140 kV/cm while BG15 116 kV/cm and BG20 125 kV/cm.

4 Discussion

The addition of glass powder to ceramics can effectively promote sinterability and reduce the sintering temperature. Therefore, many glass compositions have been employed to sinter ceramic dielectrics such as $BaTiO_3$. However, the relative permittivity of $BaTiO_3$–glass mixture can decrease because of the dilution of high dielectric constant ceramics with glass phase which generally has low dielectric constant [5]. Glass–ceramics made by controlled crystallization of glass have shown excellent dielectric properties when high volume fraction of ferroelectric phases like $BaTiO_3$ are precipitated in the glass matrix [14]. Thus, precipitation of $BaTiO_3$ crystals from glass phase by

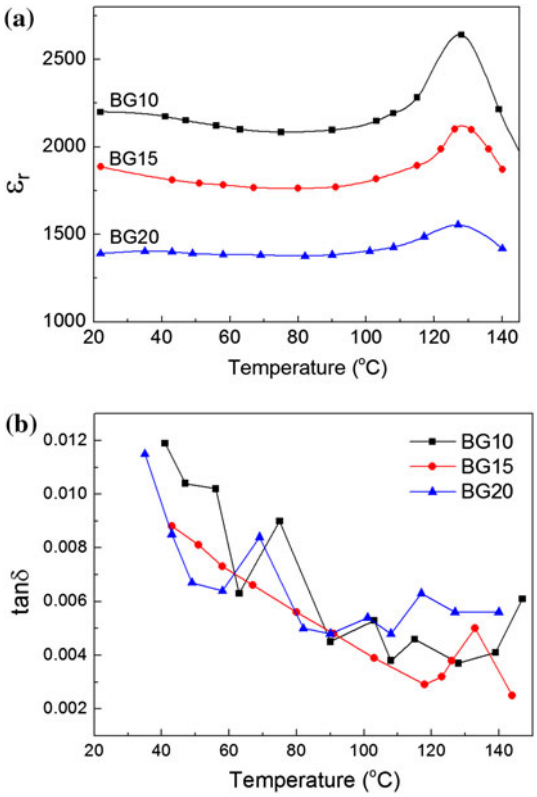

Fig. 6 **a** Relative permittivity of composites at 1 kHz as a function of temperature. **b** Loss tangent of composites at 1 kHz as a function of temperature

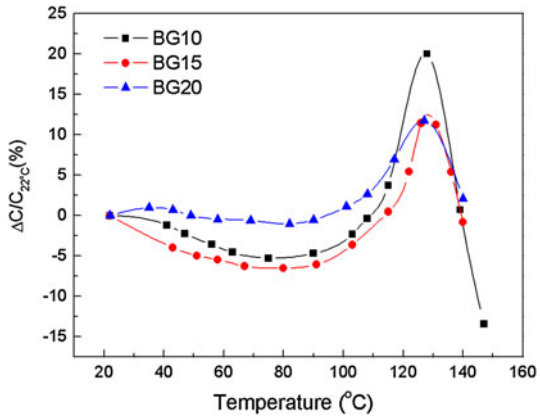

Fig. 7 Temperature coefficient of capacitance of three composites at 1 kHz

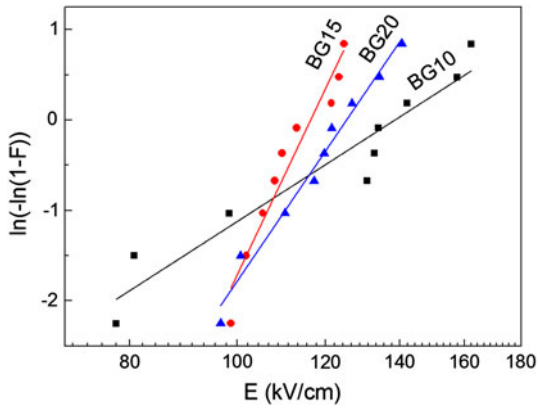

Fig. 8 Weibull plot of dielectric breakdown strength for three composites

subsequent heat-treatment can be a new approach to maintain the high dielectric constant of composites.

The following logarithmic mixing rule is often applied to describe the physical properties of composites such as dielectric constant [17],

$$\log \varepsilon = f_1 \log \varepsilon_1 + f_2 \log \varepsilon_2 \quad (5)$$

where f_1 and f_2 are the volume fraction of component 1 and component 2, respectively, and ε, ε_1 and ε_2 are the dielectric constant of the composite, component 1 and component 2, respectively. Figure 9 shows the logarithmic mixing rule fitting of dielectric constant at room temperature at 1 kHz for the composites before and after crystallization heat-treatment. Pellets without crystallization heat-treatment are prepared by cooling composites rapidly to room temperature after liquid phase sintering. The two fitting lines converge at one point where there is no glass addition, which corresponds to the dielectric constant, ~4,200, of pure $BaTiO_3$. Preliminary results of this work showed that the dielectric constant of glass at room temperature after heat-treatment at 1,000 °C for 2 h increased from 20 to 165, as shown in the inset of Fig. 9. The fitting line of composites after sintering and crystallization heat-treatment gave dielectric constant value of 53 at 100 vol% glass, which is lower than the experimental value of 165. This discrepancy was probably caused by the imperfect accuracy of logarithmic mixing rule [18, 19]. Among those samples, BG10 after sintering and crystallization has the highest dielectric constant at room temperature, approximately 2,300. Compared to the composites without crystallization heat-treatment, dielectric constant of samples after crystallization is improved significantly. Thus, we have demonstrated that the crystallizable glass did help increase dielectric constant of composites by precipitation of ferroelectric phase during crystallization heat-treatment.

For ceramic materials, the dielectric breakdown strength, like mechanical strength, is influenced by many factors, such as porosity, grain size as well as extrinsic measurement conditions (sample geometry and electrode materials) [20, 21]. Compared to bulk ceramic $BaTiO_3$ (100 kV/cm), dielectric breakdown strength of the present $BaTiO_3$/crystallizable glass composites showed only moderate improvement. This could be due to the agglomeration and growth of $BaTiO_3$ nano-powders, which leads to the non-uniform dispersion of glass powder around

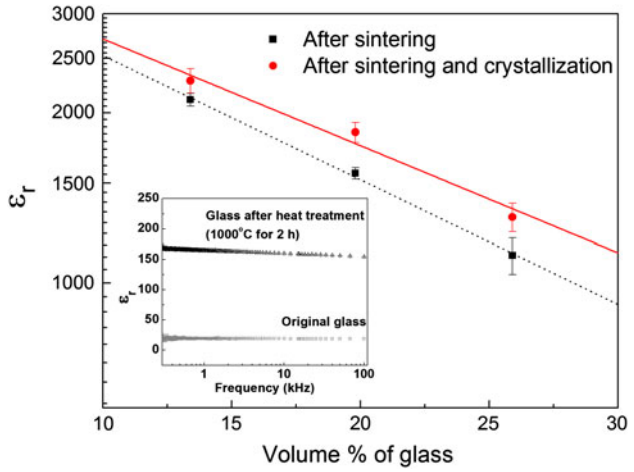

Fig. 9 Logarithmic mixing rule fitting of dielectric constant for composites before and after crystallization heat-treatment at 1,000 °C for 2 h; (*inset*) dielectric constant of glass before and after crystallization heat-treatment (1,000 °C for 2 h) as a function of frequency

$BaTiO_3$ particles. Another possible reason may be related to the sample geometry and electrode material. Previous work showed that dielectric breakdown strength depends upon the sample size such as thickness, with thinner sample giving higher breakdown strength [20–22]. It is widely accepted that an empirical power law dependence of dielectric breakdown strength, E_b, upon sample thickness, d, by $E_b \sim 1/d^n$ exhibits good agreement with experimental results [23–25]. Different values of power n ranging from 0.14 to 2.1 have been reported depending on the dielectric material and sample thickness range. Also, reduction of grain size can be another effective method to improve dielectric breakdown strength of material [10, 21]. Prevention of the grain growth during the sintering would be an important factor. Furthermore, dielectric breakdown strength varied with different electrode materials resulting from the different work functions of metals [26]. It is possible that silver, which has lower work function than Pt and Au, can lead to a higher charge injection into dielectrics and result in a lower dielectric breakdown strength.

5 Conclusion

$BaTiO_3$/crystallizable glass composites were fabricated and their dielectric properties were characterized. Samples with 10 wt% glass component have a dielectric constant around 2,300 and a dielectric breakdown strength of 140 kV/cm. Results showed that heat-treatment of samples for crystallization of glass helped improve the dielectric constant of composites significantly because of the precipitation of barium titanate from glass phase. Various methods to improve the dielectric breakdown strength of composites were considered such as uniform mixing of glass and $BaTiO_3$ powder, reduction of the grain size and tailoring extrinsic measurement conditions such as sample geometry or electrode material. We have demonstrated that crystallizable glass can be a new candidate as sintering aid for barium titanate ceramics.

Acknowledgments This research was supported by NSF-EFRI Grant 1038272. The X-ray multipurpose diffractometer used in the present research was acquired through MRI award DMR 0821536.

References

1. G. Arlt, D. Hennings, G. de With, J. Appl. Phys. **58**, 1619 (1985)
2. K. Ying, T.-E. Hsieh, Mater. Sci. Eng., B **138**, 241 (2007)
3. C. Hsi, Y. Chen, H. Jantunen, M. Wu, T. Lin, J. Eur. Ceram. Soc. **28**, 2581 (2008)
4. P.H. Fang, W.S. Brower, Phys. Rev. **113**, 456 (1959)
5. C.-H. Wang, L. Wu, Jpn. J. Appl. Phys. **32**, 2020 (1993)
6. J.C.C. Lin, W.C.J. Wei, J. Am. Ceram. Soc. **93**, 4103 (2010)
7. H. Hsiang, C. His, C. Huang, S. Fu, J. Alloys Compd. **459**, 307 (2008)
8. C. Sun, X. Wang, L. Li, Ceram. Int. **38S**, S49 (2012)
9. J.C.C. Lin, W.C.J. Wei, J. Electroceram. **25**, 179 (2010)
10. A. Young, G. Hilmas, S.C. Zhang, R.W. Schwartz, J. Am. Ceram. Soc. **90**, 1504 (2007)
11. G. Chen, Y. Yang, X. Kang, C. Yuan, C. Zhou, J. Mater. Sci. Mater. Electron. **24**, 196 (2013)
12. Q. Zhang, L. Wang, J. Luo, Q. Tang, J. Du, J. Am. Ceram. Soc. **92**, 1871 (2009)
13. V.S. Puli, D.K. Pradhan, A. Kumar, R.S. Katiyar, X. Su, C.M. Busta, M. Tomozawa, D.B. Chrisey, J. Mater. Sci.: Mater. Electron. **23**, 2005 (2012)
14. A. Herczog, J. Am. Ceram. Soc. **47**, 107 (1964)
15. A. Polotai, K. Breece, E. Dickey, C. Randall, J. Am. Ceram. Soc. **88**, 3008 (2005)
16. S. Bae, D. Yim, K. Hong, J. Park, H. Shin, H. Jung, Int. J. Appl. Ceram. Technol. **6**, 679 (2009)
17. D. McCauley, R.E. Newnham, C.A. Randall, J. Am. Ceram. Soc. **81**, 979 (1998)
18. K. Wakino, J. Am. Ceram. Soc. **76**, 2588 (1993)
19. Y. Wu, X. Zhao, F. Li, Z. Fan, J. Electroceram. **11**, 227 (2003)
20. R. Gerson, T.C. Marshall, J. Appl. Phys. **30**, 1650 (1959)
21. Y. Ye, S.C. Zhang, F. Dogan, E. Schamiloglu, J. Gaudet, P. Castro, M. Roybal, M. Joler, C. Christodoulou, in *Proceedings of 14th IEEE International Pulsed Power Conference,* 2003, pp. 719–722
22. A.D. Milliken, A.J. Bell, J.F. Scott, Appl. Phys. Lett. **90**, 112910 (2007)
23. F. Forlani, N. Minnaja, J. Vac. Sci. Technol. **6**, 518 (1969)
24. H. Lee, N.J. Smith, C.G. Pantano, E. Furman, M.T. Lanagan, J. Am. Ceram. Soc. **93**, 2346 (2010)
25. C.H. Huang, V.K. Agarwal, J. Vac. Sci. Technol., A **3**, 2000 (1985)
26. D. Wetz, J. Mankowski, J. Dickens, M. Kristiansen, in *Proceedings of 15th IEEE International Pulsed Power Conference*, 2005, pp. 935–938